IEEE Access
Multidisciplinary | Rapid Review | Open Access Journal

Received November 1, 2020, accepted November 23, 2020, date of publication November 25, 2020,
date of current version December 10, 2020.

Digital Object Identifier 10.1109/ACCESS.2020.3040494

Analytical Formulas for Wave Propagation at Low Frequencies in Half-Spaces Due to a Horizontal Magnetic Dipole

HONGLEI XU[1], (Member, IEEE), YONG ZHU[1], XIAO WEI[1], LIANGSHENG LI[1], YIN HONG-CHEN[1], AND TINGTING GU[2], (Member, IEEE)

[1]Science and Technology on Electromagnetic Scattering Laboratory, Beijing 100854, China
[2]Department of Information Science and Electronic Engineering, Innovative Institute of Electromagnetic Information and Electronic Engineering, Zhejiang University, Hangzhou 310027, China

Corresponding author: Tingting Gu (ttgu@zju.edu.cn)

This work was supported in part by the National Natural Science Foundation of China under Grant 61490695, and in part by the China Postdoctoral Science Foundation under Grant 2020M670409.

ABSTRACT The Sommerfeld Integrals (SIs) are re-visited in the presence of half-spaces under the assumption of $\gamma_0 \approx i\lambda$ being valid for low-frequency propagation in order to investigate the near-field due to a Horizontal Magnetic Dipole (HMD). Analytical expressions are derived for the excited waves over a planar homogeneous conducting ground or sea surface, and a numerical Finite Element Method (FEM) approach is also exploited to validate its correctness and effectiveness. The proposed method is additionally verified by late released experimental data, and it is shown that the results for various simplified expressions qualitatively corroborate the conclusions found in published papers. The proposed formulas can be used as a valuable tool for the study of the properties of near-field propagations from a loop antenna.

INDEX TERMS Half-space, horizontal magnetic dipole, low-frequency, lossy medium, Sommerfeld integrals.

I. INTRODUCTION

Although the National Bureau of Standards (NBS) formula recommended in 1967 [1] has been widely used for near-field measurement, which covers various frequency bands of the overall range from 30 Hz to 1000 MHz, and its recommended practice was given in 2012 [2], it seems that an effective general solution describing the near-field of a calibration antenna device is still needed to derive for providing with higher accuracies, driven by the widely applications, i.e. at some Radio Frequency Identification (RFID) frequency bands [3]–[6].

Applications of some lower RFID bands are usually found for instrument calibrations, such as the Low Frequency (LF, 120 − 150 kHz) band in [7]–[9] and High Frequency (HF, at center frequency of 13.56 MHz) band in [10]–[12], respectively. From a direct inter-comparison of experimental measurement with analytical results by Chinese researchers in [13], the authors have claimed the importance to obtain more accurate formulas, rather than segmented expressions as defined for various "quasi-static" distance ranges, to express the near-field strength decaying in some calibration systems.

It is desirable of two independent approaches at least of measuring any physical quantity, i.e. the Standard-Antenna Method (SAM) and the Standard-Field Method (SFM), consisting of generating and computing the voltage and desired component of a standard field, respectively [1]. The former consists of measuring radiation in near zone by the component of the field being evaluated, and computing the value of the field in terms of this voltage. The second method consists of generating and computing the desired component of a standard field and form of a transmitting antenna, its current distribution, the distance from the transmitting antenna to the point at which the field component is being evaluated, and the effect, if any, of the ground.

Both methods require rigorous expressions to simulate a radiating device of the magnetic field for calculating the amplitude of the magnetic field induced in a standard receiving antenna. Applications are found, for example, in studies on variation of field strength in underground mine area on the size of Very Low Frequency (VLF: 3 ∼ 30 kHz) loop antennas laid on the Earth surface or mountain [14]–[16],

The associate editor coordinating the review of this manuscript and approving it for publication was Xiaokang Yin.

covering the dimensions and form of the standard antenna, and its orientation with respect to the field vector. This old subject had been developed theoretically by investigators over the years, including the case of excitation at some height above the earth due to the launch activity of a space borne loop antenna [17], [18].

In real-life scenarios, it is of great importance to idealize the radiation source as modelled by a Hertzian HMD, especially in the estimation electromagnetic radiation by some the seismic activity, and the propagation characteristics of the Super Low Frequency (SLF: 30 $\sim$ 300 Hz) / Extremely Low Frequency (ELF: 3 $\sim$ 30 Hz) electromagnetic waves on the ground which would be released by lightening discharges. A recent study by Wang *et al.* strengthened the value of this research, which applied a speeding numerical convergence algorithm for precisely evaluation [19].

Among the techniques by which the desired component of field strength can be evaluated, two methods are mostly applied: 1) full wave simulation, being effective to solve the problem exploited in [20], [21] in calculation of the VLF / SLF electric wave propagating among the Earth-ionosphere cavity; and 2) deriving of the SIs [22], as an efficient method to evaluate wave propagation in half-spaces, which had been first released in 1909, and then, developed by Bańos and Wesley [23], Bańos [24], King *et al.* [25], Margetis [26], Margetis and Wu [27] and Collin [28] over the recent decades, respectively.

In the present study, the authors will re-visit the SIs by a good approximation with $\gamma_0 \approx \mathrm{i}\lambda$ under low-frequency condition, and derive the analytical solution for near-field propagation of a HMD source along the boundary of planar air-to-dielectric interface over a lossy medium. The study has been innovated by our latest publication [29], where a simple but efficient solution has been obtained under this assumption, in order to investigate the characteristics of near-field propagation due to a Vertical Magnetic Dipole (VMD) source.

Even though studies on this problem has been frequently addressed in the last decades analytically [30]–[32], excellent performance providing with more accuracies as exhibited in [29] would ensure the advantage of the present approach. Aside from the mathematical derivations, the present case of a HMD is different from a VMD excitation in a twofold fashion: one is about the diverse propagation behaviours for field types, and another is because of the different propagation directions. This makes the focus here is on deriving for the field component in the air-space, while the previous study is for wave penetrating in dielectric medium.

Based on above analysis, computation and discussion are carried out by equipment of the derived formulas for the near-field propagation from a HMD antenna over the planar sea surface and the time dependence $e^{\mathrm{i}\omega t}$ is suppressed throughout the analysis. The results are compared with the evaluations by the "quasi-static" formula, which had been exploited in the recent publications [35], [36], the NBS formula, with experimental data, as well as the numerical solution to prove its correctness and effectiveness.

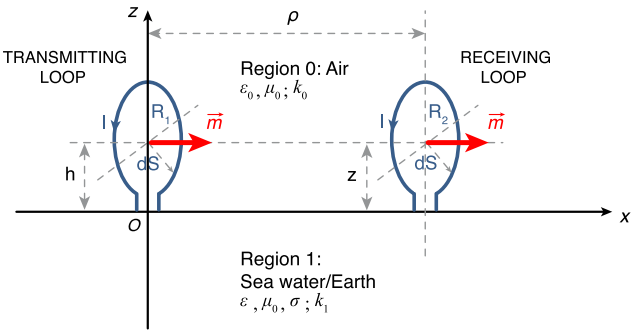

FIGURE 1. Schematic diagram and coaxial arrangement of transmitting loop antenna (radius R_1 meters), and receiving loop antenna (radius R_2 meters), spacing ρ meters.

This general approach would open a new way to obtain the simple formulas for evaluating SIs for the study of the characteristics of near-field which propagates along a planar lossy ground or sea surface, and also provide with some help and assistance to the researcher or engineer who has interest in relevant study.

II. DERIVATIONS

A. SOMMERFELD INTEGRALS IN THE PRESENCE OF HALF-SPACES FOR FIELD COMPONENTS INDUCED BY A HMD SOURCE

The geometry and notations are shown in Fig. 1, in which the upper half-space ($z \geq 0$) is Region 0 occupied by air, and the lower half-space ($z < 0$) is Region 1 being characterized as a lossy ground or sea. For each region, the wave number is defined by $k_0 = \omega/c$ and $k_1 = \sqrt{\mathrm{i}\omega\mu_0\sigma}$, respectively, in which μ_0 (the value of μ_0 is $4\pi \times 10^{-7}$ N/A^2) and ω are permeability constant and angular frequency in free space and σ is the conductivity of ground or seawater medium, respectively.

Approaching to the boundary of two regions, a couple of loop antennas are mounted at the height distances of h and z above the ground, standing for transmitting and receiving devices, respectively. In Region 0, the SIs expressing for the electromagnetic field generated by a HMD source can be used for evaluating low-frequency near-field propagation of the instrument in a cylindrical coordinate (ρ, φ, z), which can be described as follows:

$$E_{0z} = -\frac{\omega\mu_0 I\mathrm{d}S}{4\pi}\sin\varphi \times \int_0^\infty \left[\frac{e^{\mathrm{i}\gamma_0|z-h|}}{\gamma_0} + Q\frac{e^{\mathrm{i}\gamma_0(z+h)}}{\gamma_0}\right] J_1(\lambda\rho)\lambda^2\mathrm{d}\lambda, \quad (1)$$

$$E_{0\rho} = \frac{\mathrm{i}\omega\mu_0 I\mathrm{d}S}{4\pi}\sin\varphi \times \left\{\int_0^\infty \left(\pm e^{\mathrm{i}\gamma_0|z-h|} - Qe^{\mathrm{i}\gamma_0(z+h)}\right) J_0(\lambda\rho)\lambda\mathrm{d}\lambda + \int_0^\infty \frac{k_0^2 - k_1^2}{MN} e^{\mathrm{i}\gamma_0(z+h)} \cdot [J_0(\lambda\rho) + J_2(\lambda\rho)] \cdot \lambda^3\mathrm{d}\lambda\right\}; \quad \begin{cases} 0 \leq z \leq h \\ z > h, \end{cases} \quad (2)$$

$$E_{0\varphi} = \frac{\mathrm{i}\omega\mu_0 I\mathrm{d}S}{4\pi}\cos\varphi \times\left\{\int_0^\infty\left(\pm e^{\mathrm{i}\gamma_0|z-h|} - Qe^{\mathrm{i}\gamma_0(z+h)}\right)J_0(\lambda\rho)\lambda\mathrm{d}\lambda + \int_0^\infty\frac{k_0^2-k_1^2}{MN}e^{\mathrm{i}\gamma_0(z+h)}\cdot[J_0(\lambda\rho)-J_2(\lambda\rho)]\cdot\lambda^3\mathrm{d}\lambda\right\};\quad\begin{cases}0\le z\le h\\ z>h,\end{cases} \tag{3}$$

$$H_{0z} = \frac{I\mathrm{d}S}{4\pi}\cos\varphi \times\int_0^\infty\left\{\pm e^{\mathrm{i}\gamma_0|z-h|} - \left[Q-\frac{2(k_0^2-k_1^2)\lambda^2}{MN}\right]\cdot e^{\mathrm{i}\gamma_0(z+h)}\right\}J_1(\lambda\rho)\lambda^2\mathrm{d}\lambda;\quad\begin{cases}0\le z\le h\\ z>h,\end{cases} \tag{4}$$

$$H_{0\rho} = -\frac{\mathrm{i}I\mathrm{d}S}{4\pi}\cos\varphi \times\left\{-k_0^2\int_0^\infty\left[\frac{e^{\mathrm{i}\gamma_0|z-h|}}{\gamma_0}+Q\frac{e^{\mathrm{i}\gamma_0(z+h)}}{\gamma_0}\right]\cdot J_0(\lambda\rho)\lambda\mathrm{d}\lambda + \frac{1}{2}\int_0^\infty\frac{e^{\mathrm{i}\gamma_0|z-h|}}{\gamma_0}[J_0(\lambda\rho)-J_2(\lambda\rho)]\lambda^3\mathrm{d}\lambda + \frac{1}{2}\int_0^\infty\left[\frac{Q}{\gamma_0}+\frac{2(k_0^2-k_1^2)\gamma_0}{MN}\right]e^{\mathrm{i}\gamma_0(z+h)}\cdot[J_0(\lambda\rho)-J_2(\lambda\rho)]\lambda^3\mathrm{d}\lambda\right\}, \tag{5}$$

$$H_{0\varphi} = -\frac{\mathrm{i}I\mathrm{d}S}{4\pi}\sin\varphi \times\left\{-k_0^2\int_0^\infty\left[\frac{e^{\mathrm{i}\gamma_0|z-h|}}{\gamma_0}+Q\frac{e^{\mathrm{i}\gamma_0(z+h)}}{\gamma_0}\right]\cdot J_0(\lambda\rho)\lambda\mathrm{d}\lambda + \frac{1}{2}\int_0^\infty\frac{e^{\mathrm{i}\gamma_0|z-h|}}{\gamma_0}[J_0(\lambda\rho)-J_2(\lambda\rho)]\lambda^3\mathrm{d}\lambda + \frac{1}{2}\int_0^\infty\left[\frac{Q}{\gamma_0}+\frac{2(k_0^2-k_1^2)\gamma_0}{MN}\right]e^{\mathrm{i}\gamma_0(z+h)}\cdot[J_0(\lambda\rho)+J_2(\lambda\rho)]\lambda^3\mathrm{d}\lambda\right\}, \tag{6}$$

in which

$$\gamma_n = \sqrt{k_n^2-\lambda^2},\quad n=0,1. \tag{7}$$

$$N = k_1^2\gamma_0 + k_0^2\gamma_1, \tag{8}$$

$$M = \gamma_0+\gamma_1, \tag{9}$$

$$Q = \frac{k_1^2\gamma_0 - k_0^2\gamma_1}{N}. \tag{10}$$

It is noted that the square root in (7) is taken in the first quadrant, and S is the area of the transmitting loop with square meters.

B. ANALYTICAL FORMULAS EXPRESSING FIELD COMPONENTS NEAR THE BOUNDARY OF AIR-TO-DIELECTRIC INTERFACE

In the applied scenarios, the radial distance ρ between the transmitter and receiver being subjected $k_0\rho \ll 1$ satisfies the near-field condition at the operated low frequencies for various "quasi-static" distances, and the ratio of the wave numbers ensures $k_0/|k_1| \ll 1$ for lossy medium.

Usually, both the heights (h and z) of the transmitting and receiving antennas are much less than the horizontal distance ρ, i.e. $h \ll \rho$ and $z \ll \rho$. The condition of $k_0\rho \ll 1$ ensures that the main contribution of the Sommerfeld's integrals from (1) to (6) is from the path of integration where $\lambda \gg k_0$. Therefore, the following approximations are exploited in derivations.

1) AT THE "NEAR-ZONE" RANGE

It is seen the antenna of the instrument will receive the horizontal component of the magnetic field generated by a standard small loop in order to calibrate the instrument. In this case, two approximations can be inferred from $\gamma_0 \approx \mathrm{i}\lambda$, summarized as follows:

i) It leads to

$$\left|k_0^2\gamma_1\right| \ll \left|k_1^2\gamma_0\right|, \tag{11}$$

$$|\gamma_1-\gamma_0-k_1| < |k_1|. \tag{12}$$

ii) By neglecting terms of higher order $k_0^2\gamma_1/k_1^2\gamma_0$, the factor Q and $k_0 - k_1/(MN)$ may be reduced to

$$Q \approx 1, \tag{13}$$

$$\frac{k_0^2-k_1^2}{MN} \approx \frac{\gamma_0-\gamma_1}{k_1^2\gamma_0}. \tag{14}$$

Thus, the SIs defined by integrals from (1) to (6) can be simplified by using the conditions from (11) to (14), rewritten as follows:

$$E_{0z} = -\frac{\omega\mu_0 I\mathrm{d}S}{4\pi}\sin\varphi \times[F_1(k_0,d_0)+F_1(k_0,d_1)], \tag{15}$$

$$E_{0\rho} = \frac{\mathrm{i}\omega\mu_0 I\mathrm{d}S}{4\pi}\sin\varphi \left[\pm F_2(k_0,d_0) - F_2(k_0,d_1) - \frac{1}{k_1^2}F_7(d_1)\right];\quad\begin{cases}0\le z\le h\\ z>h,\end{cases} \tag{16}$$

$$E_{0\varphi} = \frac{\mathrm{i}\omega\mu_0 I\mathrm{d}S}{4\pi}\cos\varphi\cdot[\pm F_2(k_0,d_0) - F_2(k_0,d_1) - \frac{1}{k_1^2}F_8(d_1)];\quad\begin{cases}0\le z\le h\\ z>h,\end{cases} \tag{17}$$

$$H_{0z} = \frac{I\mathrm{d}S}{4\pi}\cos\varphi\cdot[\pm F_3(k_0,d_0) - F_3(k_0,d_1) + \frac{2}{k_1^2}F_9(d_1)]; \quad \begin{cases} 0\le z\le h \\ z>h, \end{cases} \tag{18}$$

$$H_{0\rho} = -\frac{\mathrm{i}I\mathrm{d}S}{4\pi}\cos\varphi\cdot\Big\{-k_0^2[F_4(k_0,d_0) + F_4(k_0,d_1)] + \frac{1}{2}[F_5(k_0,d_0) + F_5(k_0,d_1)] - \frac{1}{k_1^2}F_{10}(d_1)\Big\}, \tag{19}$$

$$H_{0\varphi} = -\frac{\mathrm{i}I\mathrm{d}S}{4\pi}\sin\varphi\cdot\Big\{-k_0^2[F_4(k_0,d_0) + F_4(k_0,d_1)] + \frac{1}{2}[F_6(k_0,d_0) + F_6(k_0,d_1)] - \frac{1}{k_1^2}F_{11}(d_1)\Big\}, \tag{20}$$

where

$$d_0 = |z-h|; \quad d_1 = z+h \tag{21}$$

$$r_0 = \sqrt{d_0^2+\rho^2}; \quad r_1 = \sqrt{d_1^2+\rho^2}. \tag{22}$$

The formulas for evaluating above expressions are developed by solving the separated integrals accordingly. In monograph by King *et al.* [25], explicit formulas are given for evaluating SIs from F_1 to F_6, which are listed in Sec. appendix. The rest integrals are to be considered, focusing on finding analytical solutions of the following integrals from F_7 to F_{11}.

2) ANALYTICAL FORMULAS FOR INTEGRALS OF F_7 AND F_8

For the electric components $E_{0\rho}$ and $E_{0\varphi}$, the integrals F_7 and F_8 in (16) and (17) are defined by:

$$F_7(d_1) = \int_0^\infty \frac{\gamma_1-\gamma_0}{\gamma_0}e^{i\gamma_0 d_1}\times[J_0(\lambda\rho)+J_2(\lambda\rho)]\,\lambda^3 d\lambda, \tag{23}$$

$$F_8(d_1) = \int_0^\infty \frac{\gamma_1-\gamma_0}{\gamma_0}e^{i\gamma_0 d_1}\times[J_0(\lambda\rho)-J_2(\lambda\rho)]\,\lambda^3 d\lambda. \tag{24}$$

respectively.

Separation of the function of $\gamma_1/\gamma_0 - 1$ in integrands in (23) and (24) in [25], analytical formulas (25) and (26) are obtained resulting from solutions of I_7, $I_{22}(\beta,z)$, I_{E} and $I_{23}(\beta,z)$ combining of formulas of D16, A22a, D5 and A23a in [25], respectively.

They are

$$F_7(d_1) = \left[2k_0\left(\frac{d_1}{r}\right)\left(\frac{k_0}{r^2}+\frac{3\mathrm{i}}{r^3}-\frac{3}{k_0 r^4}\right) - 2\mathrm{i}\left(\frac{k_0^2}{\rho^2}+\frac{3\mathrm{i}k_0}{2\rho^3}\right)\right]e^{\mathrm{i}k_0 r} + \frac{2\mathrm{i}k_1^2}{k_0\rho^3}e^{\mathrm{i}k_1\rho}e^{\mathrm{i}k_0 d_1}, \tag{25}$$

$$F_8(d_1) = \left[2k_1\left(\frac{\mathrm{i}k_1}{\rho^2}-\frac{7}{2\rho^3}\right) - 2k_0\left(\frac{d_1}{r}\right) \times\left(-\frac{\mathrm{i}k_0^2}{r}+\frac{5k_0}{r^2}+\frac{12\mathrm{i}}{r^3}-\frac{12}{k_0 r^4}\right)\right]e^{\mathrm{i}k_0 r} - 2k_1 e^{\mathrm{i}kd_1}e^{\mathrm{i}k_0\rho}\left(\frac{\mathrm{i}k_0^2}{\rho}-\frac{2k_0}{\rho^2}-\frac{2\mathrm{i}}{\rho^3}\right). \tag{26}$$

3) SIMPLIFICATION OF $(\gamma_0-\gamma_1)$ AT LOW FREQUENCIES

In accord to [29], an efficient simplification is found to be valid for radio wave propagation at low frequencies.

Use is made by follow,

$$\frac{|\gamma_0\gamma_1|}{k_0^2} \gg 1. \tag{27}$$

employed as Eq.(18) in [29], then $\frac{1}{M}$ has

$$\frac{1}{M} = \frac{\gamma_0^2-\gamma_0\gamma_1}{\gamma_0(k_0^2-k_1^2)}, \tag{28}$$

inferred from (9) with consideration of $\gamma_0^2-\gamma_1^2 = k_0^2-k_1^2$, which contributes to

$$\frac{1}{M} \approx \frac{\varepsilon}{\varepsilon-1}\frac{k_0^2}{(i\lambda)^2\gamma_1} + \frac{(\varepsilon+1)}{(\varepsilon-1)}\frac{1}{\gamma_1}, \tag{29}$$

in which

$$\gamma_0-\gamma_1 = \frac{k_0^2-k_1^2}{(\gamma_0+\gamma_1)} = \frac{k_0^2-k_1^2}{M}. \tag{30}$$

is applied.

4) ANALYTICAL FORMULAS FOR INTEGRALS FROM F_9 TO F_{11}

For the three magnetic components H_{0z}, $H_{0\rho}$ and $H_{0\varphi}$, the integrals from F_9 to F_{11} in equations from (18) to (20) are defined, accordingly

$$F_9(d_1) = \int_0^\infty \gamma_0(\gamma_1-\gamma_0)e^{i\gamma_0 d_1}J_1(\lambda\rho)\lambda^2 d\lambda, \tag{31}$$

$$F_{10}(d_1) = \int_0^\infty (\gamma_1-\gamma_0)e^{i\gamma_0 d_1} \times[J_0(\lambda\rho)-J_2(\lambda\rho)]\,\lambda^3 d\lambda, \tag{32}$$

$$F_{11}(d_1) = \int_0^\infty (\gamma_1-\gamma_0)e^{i\gamma_0 d_1} \times[J_0(\lambda\rho)+J_2(\lambda\rho)]\,\lambda^3 d\lambda. \tag{33}$$

Substituting (29) into (30), then, replacing the function $(\gamma_1-\gamma_0)$ in the integrands of equations from (31) to (33), it yields,

$$F_9(d_1) = -\frac{\varepsilon\rho k_0^4}{2}\left(\frac{\mathrm{i}}{k_0\rho^3}-\frac{d_1}{\rho^3}+\frac{2k_0}{k_1\rho^2}\right)e^{\mathrm{i}k_0 d_1} + \left[\frac{\varepsilon k_0^5}{k_1\rho}-(\varepsilon+1)k_0^3\left(\frac{k_1}{\rho}+\frac{\mathrm{i}}{\rho^2}\right)\right]e^{\mathrm{i}k_1\rho}e^{\mathrm{i}k_0 d_1} - \left[\frac{\varepsilon k_0^3}{\rho^2}-(\varepsilon+1)k_0^2\left(\frac{k_0}{\rho^2}+\frac{3\mathrm{i}}{2\rho^3}\right)\right]e^{\mathrm{i}k_0 r} \tag{34}$$

$$F_{10}(d_1) = -2k_0^3 d_1 \left[\frac{\varepsilon+1}{r}\left(\frac{k_0}{\rho} + \frac{3\mathrm{i}}{2\rho^2} - \frac{5}{8k_0\rho^3}\right) + \varepsilon k_0 \left(\frac{1}{\rho^2} + \frac{\mathrm{i}}{2k_0\rho^3} + \frac{3}{8k_0^2\rho^4}\right)\right] e^{\mathrm{i}k_0 r} - \frac{2\varepsilon k_0^4}{\rho^2}\left(\frac{d_1}{k_0\rho} - \frac{1}{k_1}\right) e^{\mathrm{i}k_0 d_1} + 2k_0^2 \left[\varepsilon k_0^2 \left(\frac{\mathrm{i}}{\rho} - \frac{1}{k_1\rho^2}\right) - (\varepsilon+1)\left(\frac{\mathrm{i}k_1^2}{\rho} - \frac{2k_1}{\rho^2} - \frac{2\mathrm{i}}{\rho^3}\right)\right] e^{\mathrm{i}k_1\rho} e^{\mathrm{i}k_0 d_1} \quad (35)$$

$$F_{11}(d_1) = -\frac{\mathrm{i}d_1}{\rho}\left[\frac{\varepsilon k_0}{\rho^2} - 2(\varepsilon+1)\left(\frac{k_0}{\rho^2} + \frac{3\mathrm{i}}{2\rho^3}\right)\right] e^{\mathrm{i}k_0 r} - \frac{2}{\rho^2}\left[(\varepsilon+1)\left(k_1 + \frac{\mathrm{i}}{\rho}\right) - \frac{\varepsilon k_0^2}{k_1}\right] \times e^{\mathrm{i}k_1\rho} e^{\mathrm{i}k_0 d_1} - \frac{2\varepsilon k_0^4}{k_1\rho^2} e^{\mathrm{i}k_0 d_1} \quad (36)$$

by which the formulas are obtained where integrals are partitioned by several integrations addressed in [25]. Specifically, practice is made by: D4, D1, I_{D} and I_{A} for $F_9(d_1)$; D9, D13, I_{K} and I_{Q} for $F_{10}(d_1)$; D11, D14, I_{M} and I_{R} for $F_{11}(d_1)$, respectively.

Based on the above analysis, the analytical formulas have been derived readily for near-field propagation of a HMD (representing for a loop antenna) in the presence of half-spaces.

5) THE APPLIED LOW FREQUENCY RANGES AND SIMPLIFIED EXPRESSIONS

It should be clarified that the applied operating low frequencies are subjected to below restriction [29]:

$$X^*(\frac{\sigma}{\omega}) = 3.362142174 \times 10^5 \sqrt{\frac{\sigma}{\omega}} \gg 10. \quad (37)$$

to guarantee the effectiveness of (27).

Generally speaking, the amplitude of a low frequency electromagnetic wave near the ground depends on the ground conductivity, the operating frequency, and the propagation distance.

When the antennas of the transmitter and the receiver are located on the ground, we have $d_m = 0$ and $r_m = \rho$. It is seen that the high-order terms of $k_0\rho$ and $k_1\rho$ can be neglected. Specifically, the six field components in Region 0 can be derived readily. The derived formulas are subjected to the following simplified form under the assumption, written as follows:

$$E_{0z} = -\frac{\omega\mu_0 I\mathrm{d}S}{2\pi}\sin\varphi F_1, \quad (38)$$

$$E_{0\rho} = -\frac{\mathrm{i}\omega\mu_0 I\mathrm{d}S}{4\pi k_1^2}\sin\varphi F_7, \quad (39)$$

$$E_{0\varphi} = -\frac{\mathrm{i}\omega\mu_0 I\mathrm{d}S}{4\pi k_1^2}\cos\varphi F_8, \quad (40)$$

$$H_{0z} = \frac{I\mathrm{d}S}{4\pi}\cos\varphi\frac{2}{k_1^2}F_9, \quad (41)$$

$$H_{0\rho} = -\frac{\mathrm{i}I\mathrm{d}S}{4\pi}\cos\varphi\left(-2k_0^2 F_4 + F_5 - \frac{1}{k_1^2}F_{10}\right), \quad (42)$$

$$H_{0\varphi} = -\frac{\mathrm{i}I\mathrm{d}S}{4\pi}\sin\varphi\left(-2k_0^2 F_4 + F_6 - \frac{1}{k_1^2}F_{11}\right), \quad (43)$$

in which the simplified integrals can be solved correspondingly, as follows:

$$F_1 = -\left(\frac{k_0}{\rho} + \frac{\mathrm{i}}{\rho^2}\right)e^{\mathrm{i}k_0\rho}, \quad (44)$$

$$F_4 = -\frac{\mathrm{i}e^{\mathrm{i}k_0\rho}}{\rho}, \quad (45)$$

$$F_5 = -2k_0\left(\frac{\mathrm{i}k_0}{\rho} - \frac{2}{\rho^2} - \frac{2\mathrm{i}}{k_0\rho^3}\right)e^{\mathrm{i}k_0\rho}, \quad (46)$$

$$F_6 = -2k_0\left(\frac{1}{\rho^2} + \frac{\mathrm{i}}{k_0\rho^3}\right)e^{\mathrm{i}k_0\rho}, \quad (47)$$

$$F_7 = -2\mathrm{i}\left(\frac{k_0^2}{\rho^2} + \frac{3\mathrm{i}k_0}{2\rho^3}\right)e^{\mathrm{i}k_0\rho} + \frac{2\mathrm{i}k_1^2}{k_0\rho^3}e^{\mathrm{i}k_1\rho}, \quad (48)$$

$$F_8 = 2k_1\left(\frac{\mathrm{i}k_1}{\rho^2} - \frac{7}{2\rho^3}\right)e^{\mathrm{i}k_0\rho} - 2k_1 e^{\mathrm{i}k_0\rho}\left(\frac{\mathrm{i}k_0^2}{\rho} - \frac{2k_0}{\rho^2} - \frac{2\mathrm{i}}{\rho^3}\right), \quad (49)$$

$$F_9 = -\frac{\varepsilon k_0^4}{2}\left(\frac{\mathrm{i}}{k_0\rho^2} + \frac{2k_0}{k_1\rho}\right) + \left[\frac{\varepsilon k_0^5}{k_1\rho} - (\varepsilon+1)k_0^3\left(\frac{k_1}{\rho} + \frac{\mathrm{i}}{\rho^2}\right)\right]e^{\mathrm{i}k_1\rho} - \left[\frac{\varepsilon k_0^3}{\rho^2} - (\varepsilon+1)k_0^2\left(\frac{k_0}{\rho^2} + \frac{3\mathrm{i}}{2\rho^3}\right)\right]e^{\mathrm{i}k_0\rho}, \quad (50)$$

$$F_{10} = \frac{2\varepsilon k_0^4}{k_1\rho^2} + 2k_0^2\left[\varepsilon k_0^2\left(\frac{\mathrm{i}}{\rho} - \frac{1}{k_1\rho^2}\right) - (\varepsilon+1)\left(\frac{\mathrm{i}k_1^2}{\rho} - \frac{2k_1}{\rho^2} - \frac{2\mathrm{i}}{\rho^3}\right)\right]e^{\mathrm{i}k_1\rho}, \quad (51)$$

$$F_{11} = -\frac{2}{\rho^2}\left[(\varepsilon+1)\left(k_1 + \frac{\mathrm{i}}{\rho}\right) - \frac{\varepsilon k_0^2}{k_1}\right]e^{\mathrm{i}k_1\rho} - \frac{2\varepsilon k_0^4}{k_1\rho^2}. \quad (52)$$

with $z \approx h = 0$ and $d_0 = d_1 = 0$.

C. SIMPLIFIED EXPRESSIONS OF NEAR-FIELD PROPAGATION OF A HMD ANTENNA

At short propagation distances, the derived formulas can be simplified defined by equations from (48) to (52) according to the following approximations:

$$e^{\mathrm{i}k_0\rho} \approx 1 + \mathrm{i}k_0\rho - (k_0\rho)^2/2, \quad (53)$$

$$e^{\mathrm{i}k_1\rho} \approx 1 + \mathrm{i}k_1\rho - (k_1\rho)^2/2. \quad (54)$$

TABLE 1. Expressions subjected to various conditions of six electromagnetic components for low-frequency near-field propagation due to a HMD excitation, assuming the parameters are taken as $IdS = 1$, $d = h = 0^+$ and $\varphi = \pi/4$, respectively.

$4\sqrt{2}\pi \times$	$\lvert k_0\rho\rvert \ll 1$ (A)	$\lvert k_1\rho\rvert \gg 1$ (B)	Resulting Formulas (C)
E_{0z}	$2\mathrm{i}\omega\mu_0\frac{1}{\rho^2}$	$2\mathrm{i}\omega\mu_0\frac{1}{\rho^2}$	$-2\omega\mu_0 F_1$
$E_{0\rho}$	$2\mathrm{i}\omega\mu_0\frac{1}{\rho^2}$	$-2\omega\mu_0\frac{1}{k_1\rho^3}$	$-\mathrm{i}\omega\mu_0\frac{1}{k_1^2}F_7$
$E_{0\varphi}$	$-2\mathrm{i}\omega\mu_0\frac{1}{\rho^2}$	$4\omega\mu_0\frac{1}{k_1\rho^3}$	$-\mathrm{i}\omega\mu_0\frac{1}{k_1^2}F_8$
H_{0z}	$\mathrm{i}k_1\frac{1}{\rho^2}$	$-6\mathrm{i}\frac{1}{k_1\rho^4}$	$\frac{2}{k_1^2}F_9$
$H_{0\rho}$	$2\frac{1}{\rho^3}$	$4\frac{1}{\rho^3}$	$2\mathrm{i}k_0^2F_4 - \mathrm{i}F_5 + \frac{\mathrm{i}}{k_1^2}F_{10}$
$H_{0\varphi}$	$-\frac{1}{\rho^3}$	$-2\frac{1}{\rho^3}$	$2\mathrm{i}k_0^2F_4 - \mathrm{i}F_6 + \frac{\mathrm{i}}{k_1^2}F_{11}$

1) CURVE A: $k_0\rho \ll 1$

In this case, the propagation distance is assumed to be in the region of $k_0\rho \ll 1$, where the amplitude of the magnetic field probably be approximated by the static field with $k_0\rho = \frac{\rho}{c}\omega \to 0$. Thus, the integrals are solved accordingly, as follows: $F_7(0) \approx -\frac{2k_1^2}{\rho^2}$, $F_8(0) \approx \frac{2k_1^2}{\rho^2}$, $F_9(0) \approx \frac{\mathrm{i}k_1^3}{2\rho^2}$, $F_{10}(0) \approx \frac{2\mathrm{i}k_1^2}{\rho^3}$ and $F_{11}(0) \approx -\frac{\mathrm{i}k_1^2}{\rho^3}$, respectively. The applied range had previously been defined by "*quasi-near range*" in [30].

2) CURVE B: $|k_1\rho| \gg 1$

In this case, the propagation distance is assumed to in the region of $|k_1\rho| \gg 1$ yielding $e^{\mathrm{i}k_1\rho} \approx 0$, for the reason that the parameter of $\Im m(k_1\rho)$ will be great.

Additionally, the wave number k_0 in the air is very small, so that the parameter $|k_0\rho|$ is small. Therefore, we have $e^{ik_0\rho} \approx 1$. This furnishes $F_7(0) \approx -\frac{2\mathrm{i}k_1}{\rho^3}$, $F_8(0) \approx \frac{4\mathrm{i}k_1}{\rho^3}$, $F_9(0) \approx -\frac{3\mathrm{i}k_1}{\rho^4}$, $F_{10}(0) \approx -\frac{24\mathrm{i}}{\rho^5}$, and $F_{11}(0) \approx \frac{6\mathrm{i}}{\rho^5}$, respectively.

It is noted that the propagation distance with

$$|k_1\rho| = \omega\sqrt{\mu_0\sigma/2} \approx \frac{\rho}{\delta}\sqrt{\omega}, \tag{55}$$

in Region 1 is subjected to the value of the *skin depth*, defined by follow:

$$\delta = \sqrt{\frac{2}{\omega\mu_0\sigma}} \approx 503.2921 \times \frac{1}{\sqrt{f\sigma}}. \tag{56}$$

3) CURVE C

Considering that $F_7 \sim F_{11}$ can be reduced to the final approximated formulas for the six components of the electromagnetic field, summarization is found in Tab. 1. Specifically, it can be deduced that the resulted formula C for each component would be in consistent with the *quasi-static* field results for A.

III. COMPUTATION

To validate the effectiveness of the derived formulas, the values of magnitudes for the magnetic field component $H_{0\varphi}$ are plotted in Fig. 2 by various comparable results, in which the discrete measured data are taken from a recent near-field experiment released in [13] conducted by Chinese researcher and the rest curve lines are obtained by analytical formulas by using the NBS's formula in [1] with the radiating radius is taken as $R_0 = \sqrt{d^2 + R_1^2 + R_2^2}$, and the approximated solutions by A, B, C, respectively.

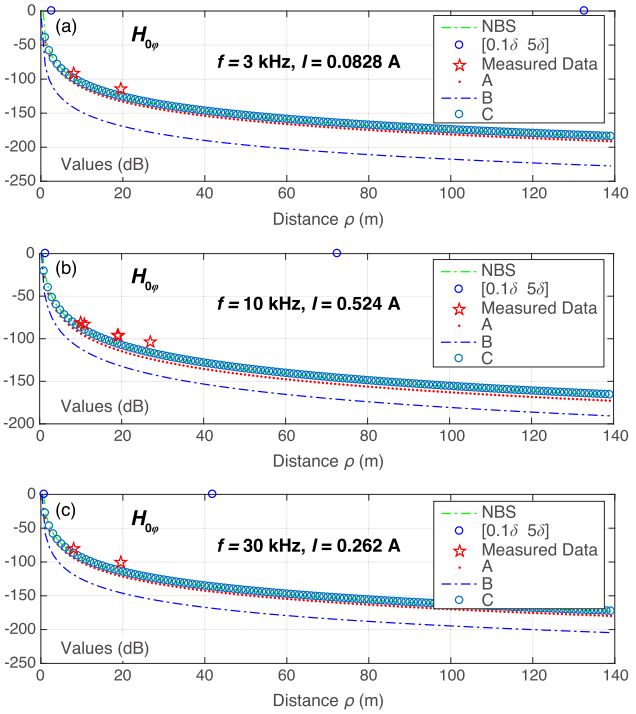

FIGURE 2. The computed and measured values of the magnetic component $H_{0\varphi}$ in near-zone from a calibration instrumental loop antenna. The NBS formula is given by $|H_{av}| \approx IS_1/(2\pi R_0^3)$, and comparative values of various simplifications marked by A, B, C, respectively (S_1 denotes the area of the first transmitting loop).

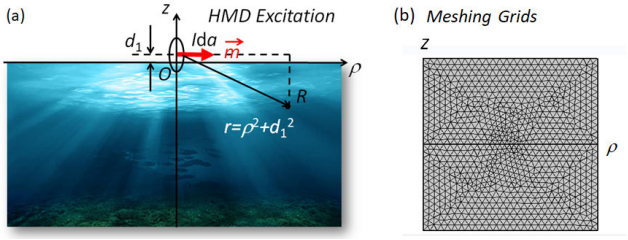

FIGURE 3. 2-D numerical modeling of near-field propagation by FEM, which is generated by a loop antenna exposed in the air (the excitation is taken by $Ida = 1$) with (a) the realistic model, and (b) meshing grids by arbitrary triangular elements with PML boundary, respectively.

A. NEAR-FIELD CALIBRATIONS

This experiment data are taken from recorded in literature [13], in which the conductivity is measured as 0.12 S/m by GMS-07e. The height of the transmitting loop is 0.3 m ($R_1 = 0.2$ m; 16 turns) and the receiving rod is placed on the ground, i.e. $z = 0$. The sensor of the receiver ($R_2 =$

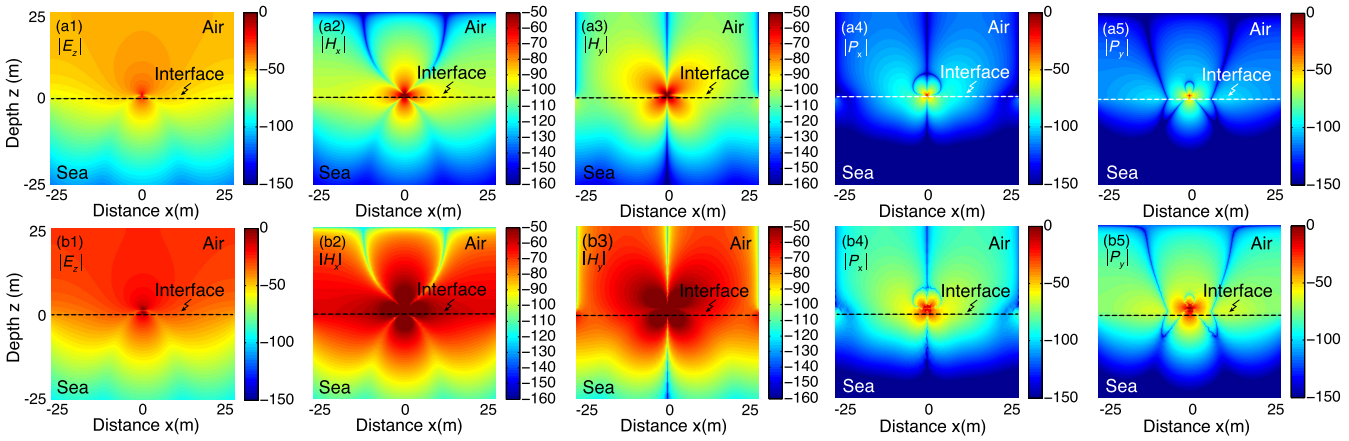

FIGURE 4. Numerical performances by full-wave simulation in half-spaces simulating the near-field propagation due to a HMD excitation at the operating frequency of $f = 3$ kHz, in which the excited source is placed at $d = 1$ m and the relative permittivity and conductivity are chosen as $\varepsilon = 80$ and $\sigma = 4$S/m with meshing sizes by (a) 0.2 × 0.2(m^2), and (b) 2 × 2(m^2), respectively.

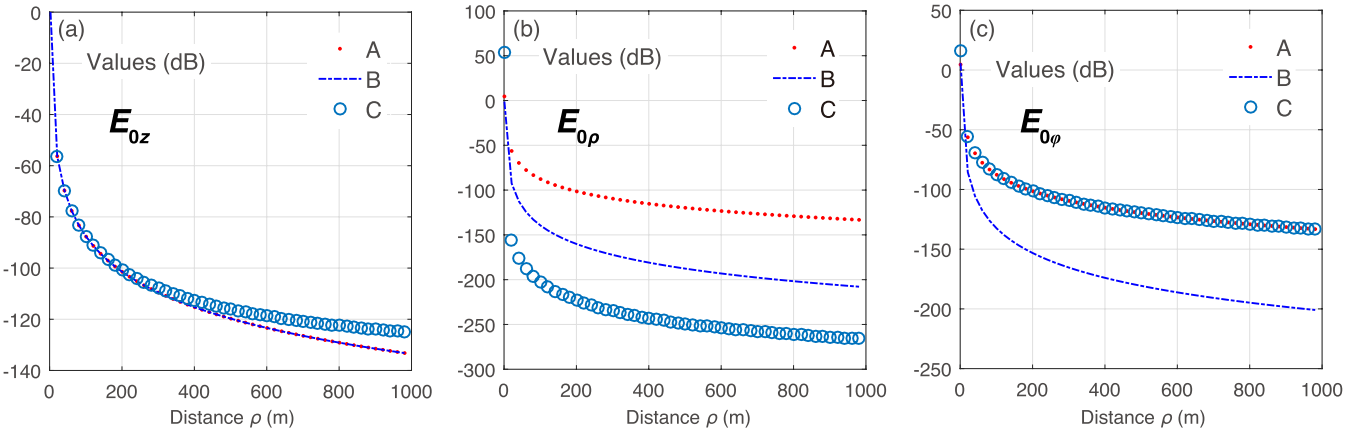

FIGURE 5. The values of E_{0z}, $E_{0\rho}$ and $E_{0\varphi}$ expressing for the electric components (in dB) in near-zone from a HMD source computed by various formulas (marked by A, B and C, respectively) under different near-field approximations of low-frequency propagation at the operating frequency $f = 50$ kHz with $d = h = 0^+$, and the relative permittivity and conductivity of lossy medium are taken as $\varepsilon = 80$, $\sigma = 4$ S/m, respectively, and $\varphi = \pi/2$, $\varphi = \pi/2$, $\varphi = 0$, respectively.

0.03775 m; 1.2 m length). The excitations are taken as chosen by $I = 0.0828, 0.524, 0.262$ amperes at various operating frequencies $f = 3, 10, 30$ kHz, respectively. It can be seen from Fig. 2 that the calculated results of derived formulas are basically consistent with the measured data and within a reasonable error range.

B. THE FULL-WAVE SIMULATION

Moreover, a full-wave simulation of the presented model in Fig. 3 (a) is given by a FEM (Finite Element Method). The meshing grids are chosen aribitrary by triangular elements as shown in Fig. 3 (b). The comparison of time consuming for the full-wave simulation and analytical solution are given in Tab.2. Calculation in Fig. 4 give the amplitudes of the field components taken by the numerical method. However, the accuracies are also subjected to different mesh sizes, as illustrated in Figs.4 (a) and 4 (b). The result in Fig. 4 reveals some discrepancies in magnitudes of field components where the error is subjected to different mesh sizes. It is noted that the calculated results with the numerical method are not stable, however, the analytical formulas proposed in this paper does not have such a problem.

C. THE ADVANTAGES

With same conditions, we compared the analytical formula, and the corresponding various simplified expressions found in published papers in Tab. 1 expressed as A, B, C, respectively. The values of magnitudes to the propagation distance ρ are computed and plotted in Fig. 5 and Fig. 6, respectively, at the operating frequency $f = 50$ kHz and the conductivity and the relative permittivity of seawater are chosen as $\sigma = 4$ S/m, and $\varepsilon = 80$, respectively. It is seen that the strength of electromagnetic components decays as the propagation distances increase in different rates. It should be pointed out that the quasi-static formulas are believed to be accurate for a long time even though the available expressions are not complete for all components. For example, the formula for the component $E_{0\rho}$ is not available for evaluation [30]. In the

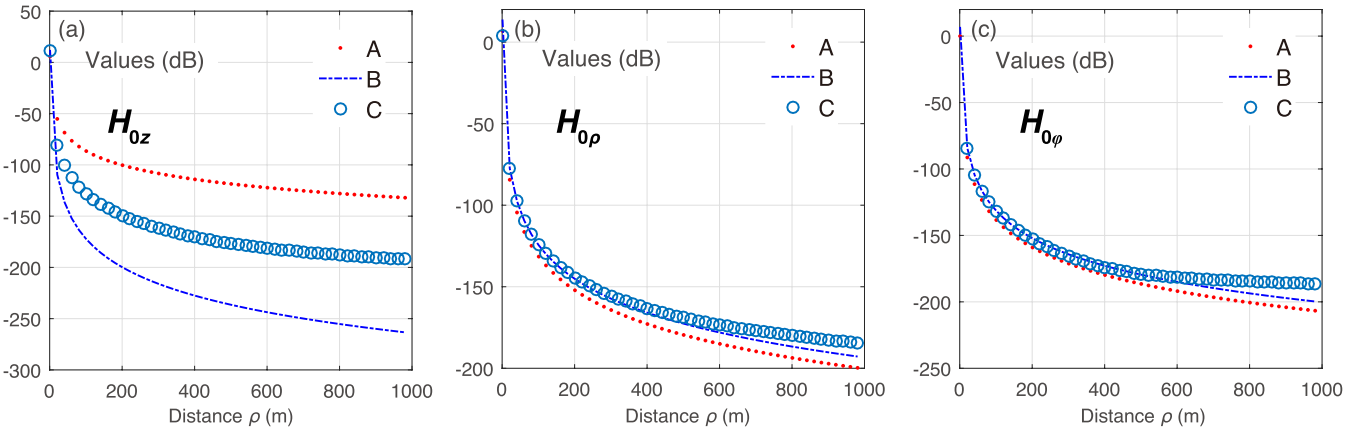

FIGURE 6. The values of H_{0z}, $H_{0\rho}$ and $H_{0\varphi}$ expressing for the magnetic components (in dB) in near-zone from a HMD source computed by various formulas (marked by A, B and C, respectively) under different near-field approximations of low-frequency propagation at the operating frequency $f = 50$ kHz with $d = h = 0^+$, and the relative permittivity and conductivity of lossy medium are taken as $\varepsilon = 80$, $\sigma = 4$ S/m, respectively, and $\varphi = 0$, $\varphi = 0$, $\varphi = \pi/2$, respectively.

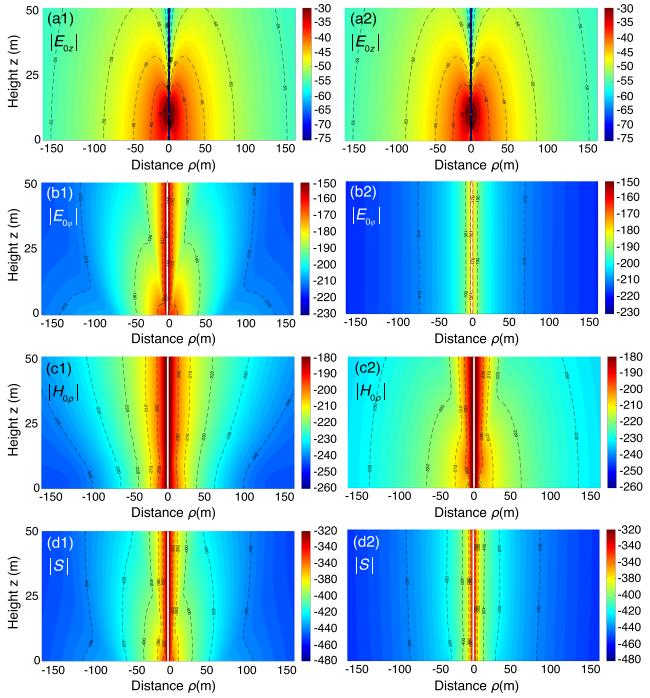

FIGURE 7. Field strength of near-field propagation at the operating frequency of $f = 50$ kHz over the ground condition of (1) dry ground surface ($\sigma = 10^{-4}$ S/m); (2) plane sea surface ($\sigma = 4$ S/m), respectively.

TABLE 2. Time consuming for various element sizes by FEM and analytical solution at the operating frequency $f = 50$ kHz, assuming the parameters are taken as $IdS = 1$, $d = 0.5$ m $\varepsilon = 4$, and $\sigma = 10^{-4}$ respectively.

Mesh size	Max: 20 m Min: 0.5 m (Coarse)	Max: 2 m Min: 5 cm (Middle)	Max: 0.2 m Min: 5 mm (Fine)
Calculation Area (CA in m^2)	20k ×20k	20k ×20k 1k × 1k 100 ×100	100 × 100
Element Units	2, 737, 742	Too much 665, 502 7, 014	653, 110
Boundary Units (Max/sqrt[CA])	5, 217(1‰)	−− (0.1‰) 2, 532(2‰) 264(20‰)	2, 500(2‰)
Degree of Freedom	19, 172, 195	Too much 4, 662, 515 49, 499	4, 575, 771
Time Full-wave Solution	535 s	> 30 min 115 s 3 s	112 s
Time Analytical Solution	< 1 s	< 1 s	< 1 s

comparisons from Fig. 5 and Fig.6 by the derived formulas with that by quasi-static approach addressed in 1964 by Durrani, the derived formulas are in accord with the available results by the quasi-static formulas to prove its effectiveness and correctness.

When the observation point is chosen arbitrarily on the $\hat{x}-\hat{z}$ plane, the distributions of the three components strength for ELF wave are depicted in Figs. 7 (a), (b) and (c), respectively. As an extension of the study, the Poynting trajectories are also plotted in Fig. 7 (d), at the operating frequency $f = 50$ kHz. In the computations, the conductivity and relative dielectric constant of the rock medium is chosen as approximately $\sigma = 10^{-4}$ S/m, and $\varepsilon = 4$ in the left column, respectively, and the conductivity and relative dielectric constant of seawater medium are taken as $\sigma = 4$ S/m, and $\varepsilon = 80$ in the right column, respectively.

The plotted distribution with Poynting trajectory in Fig.7 depicted the energy flow near the surface of the lossy ground, which shows that the ground condition has slight influence to the near-field propagation performance

IV. CONCLUSION

The study is to derive the SIs in half-spaces due to a HMD, and it gives some illustrative numerical evaluations by the obtained formulas, which could be seen as a valuable tool for the study of the properties of near-field propagation. The resulted magnetic field strength coincides with those obtained by using the NBS's formulas, FEM solution, and also with the measured experiment.

Providing with approximated results under different conditions, it may summarized in Tab. 1. We compared the properties of near-field propagation at low frequencies by various propagation distance conditions: 1) the *"quasi-static"* field region is defined by $k_0\rho \ll 1$, typically, when the horizontal distance ρ between the observer and the source dipole is less than 0.1 times of the skin depth δ of the lossy medium; 2) when it subjected to $|k_1\rho| \gg 1$, the lossy ground medium behaves as a *perfect conductive reflector*; and 3) for a more general case, we propose a approximation of $|k_0k_1|/\gamma_0^2 \gg 1$ is valid for near-field propagations at a wide frequency-band of low frequencies, which corresponds to conductivity of the ground medium, respectively. In future work, the proposed method may be utilized in more applications, such as the application environment of deep underground exploration, or submarine prospection and communication.

APPENDIX

In evaluation of the Fourier-Bessel representations of integrals from F_1 to F_6, the following expressions of identities have been derived previously in the monograph [25] by King *et al*, written by:

$$F_1(k_n, d_m) = \int_0^\infty \frac{e^{\mathrm{i}\gamma_n d_m}}{\gamma_n} J_1(\lambda\rho)\lambda^2 \mathrm{d}\lambda = -\rho k_n \left(\frac{1}{r_{m^2}} + \frac{\mathrm{i}}{k_n r_{m^3}}\right) e^{\mathrm{i}k_n r_m}, \tag{I.1}$$

$$F_2(k_n, d_m) = \int_0^\infty e^{\mathrm{i}\gamma_n d_m} J_0(\lambda\rho)\lambda \mathrm{d}\lambda = -\frac{d_m}{r_m}\left(\frac{\mathrm{i}k_n}{r_m} - \frac{1}{r_m^2}\right) e^{\mathrm{i}k_n r_m}, \tag{I.2}$$

$$F_3(k_n, d_m) = \int_0^\infty e^{\mathrm{i}\gamma_n d_m} J_1(\lambda\rho)\lambda^2 \mathrm{d}\lambda = -\rho k_n \frac{d_m}{r_m}\left(\frac{k_n}{r_m^2} + \frac{3\mathrm{i}}{r_m^3} - \frac{3}{k_n r_m^4}\right) e^{\mathrm{i}k_n r_m}, \tag{I.3}$$

$$F_4(k_n, d_m) = \int_0^\infty \frac{e^{\mathrm{i}\gamma_n d_m}}{\gamma_n} J_0(\lambda\rho)\lambda \mathrm{d}\lambda = -\frac{\mathrm{i}e^{\mathrm{i}k_n r_m}}{r_m}, \tag{I.4}$$

$$F_5(k_n, d_m) = \int_0^\infty \frac{e^{\mathrm{i}\gamma_n d_m}}{\gamma_n} \left[J_0(\lambda\rho) - J_2(\lambda\rho)\right] \lambda^3 \mathrm{d}\lambda, = -2k_n \left[\frac{\mathrm{i}k_n}{r_m} - \frac{2}{r_m^2} - \frac{2\mathrm{i}}{k_n r_m^3} - \frac{d_m^2}{r_m^2}\left(\frac{\mathrm{i}k_n}{r_m} - \frac{3}{r_m^2} - \frac{3\mathrm{i}}{k_n r_m^3}\right)\right] e^{\mathrm{i}k_n r_m}, \tag{I.5}$$

$$F_6(k_n, d_m) = \int_0^\infty \frac{e^{\mathrm{i}\gamma_n d_m}}{\gamma_n} \left[J_0(\lambda\rho) + J_2(\lambda\rho)\right] \lambda^3 \mathrm{d}\lambda = -2k_n \left(\frac{1}{r_m^2} + \frac{\mathrm{i}}{k_n r_m^3}\right) e^{\mathrm{i}k_n r_m}, \tag{I.6}$$

with $m = 0, 1$ and $n = 0, 1$, respectively.

ACKNOWLEDGMENT

The authors would like to thank Dr. Huai-Yun Peng *et al* at China Research Institute of Radio Propagation, Qingdao, Shandong, China, for providing with the experimental data. They also thank all editors and reviewers for helpful comments and suggestions.

REFERENCES

[1] F. M. Greene, "NBS field-strength standards and measurements (30 Hz to 1000 MHz)," *Proc. IEEE*, vol. 55, no. 6, pp. 970–980, Jun. 1967, doi: 10.1109/PROC.1967.5711.
[2] *IEEE Recommended Practice for Near-Field Antenna Measurements*, Standard 1720-2012, Dec. 2012.
[3] J. A. Russer, N. Uddin, A. S. Awny, A. Thiede, and P. Russer, "Near-field measurement of stochastic electromagnetic fields," *IEEE Electromagn. Compat. Mag.*, vol. 4, no. 3, pp. 79–85, Sep. 2015, doi: 10.1109/MEMC.2015.7336761.
[4] R. J. Pogorzelski, "An effective method of isolating portions of a radiator in near-field or far-field antenna measurements [Measurements Corner]," *IEEE Antennas Propag. Mag.*, vol. 55, no. 3, pp. 156–168, Jun. 2013, doi: 10.1109/MAP.2013.6586646.
[5] Y. Zeng, Z. N. Chen, X. Qing, and J.-M. Jin, "A directional, closely spaced Zero-Phase-Shift-Line loop array for UHF near-field RFID reader antennas," *IEEE Trans. Antennas Propag.*, vol. 66, no. 10, pp. 5639–5642, Oct. 2018, doi: 10.1109/TAP.2018.2860619.
[6] Y. Sim Ong, X. Qing, C. Khan Goh, and Z. Ning Chen, "A segmented loop antenna for UHF near-field RFID," in *Proc. IEEE Antennas Propag. Soc. Int. Symp.*, Toronto, ON, Canada, Jul. 2010, pp. 1–4.
[7] D. Ciudad Rio-Perez, P. C. Arribas, C. Aroca, and P. Sanchez, "Testing thick magnetic shielding effect on a new low frequency RFIDs system," *IEEE Trans. Antennas Propag.*, vol. 56, no. 12, pp. 3838–3843, Dec. 2008, doi: 10.1109/TAP.2008.2007389.
[8] J. W. Wallace, L. C. Diamantides, K. C. Ki, and M. W. Butler, "Switched-antenna low-frequency (LF) radio-frequency identification (RFID) for ornithology," *IEEE J. Radio Freq. Identif.*, vol. 4, no. 2, pp. 137–145, Jun. 2020, doi: 10.1109/JRFID.2020.2971534.
[9] C. Jebali and A. B. Kouki, "Read Range/Rate improvement of an LF RFID-based tracking system," *IEEE J. Radio Freq. Identif.*, vol. 2, no. 2, pp. 73–79, Jun. 2018, doi: 10.1109/JRFID.2018.2845669.
[10] G. Xiao, Z. Zhang, H. Fukutani, Y. Tao, and S. Lang, "Improving the *Q*-factor of printed HF RFID loop antennas on flexible substrates by condensing the microstructures of conductors," *IEEE J. Radio Freq. Identif.*, vol. 2, no. 2, pp. 111–116, Jun. 2018, doi: 10.1109/JRFID.2018.2854264.
[11] S. Rizkalla, R. Prestros, and C. F. Mecklenbrauker, "Optimal card design for non-linear HF RFID integrated circuits with guaranteed standard-compliance," *IEEE Access*, vol. 6, pp. 47843–47856, 2018, doi: 10.1109/ACCESS.2018.2867290.
[12] B. Qu, H. Liu, Q. Ye, Y. Geng, T.-L. Ren, H. Wei, and X. Han, "A novel MEMS-based 13.56 MHz microantenna for RFID applications," *IEEE Trans. Magn.*, vol. 51, no. 11, pp. 1–3, Nov. 2015, doi: 10.1109/TMAG.2015.2456156.
[13] H.-Y. Peng, Y. Chen, Y.-X. Wang, S.-T. Zhang, and Y.-Z. Mao, "Low frequency fields excited by a horizontal magnetic dipole near boundary of lossy half-space," in *Proc. 12th Int. Symp. Antennas, Propag. EM Theory (ISAPE)*, Hangzhou, China, Dec. 2018, pp. 1–4.
[14] R. Barr, W. Ireland, and M. J. Smith, "ELF, VLF and LF radiation from a very large loop antenna with a mountain core," *IEE Proc. H Microw., Antennas Propag.*, vol. 140, no. 2, pp. 129–134, Apr. 1993, doi: 10.1049/ip-h-2.1993.0020.
[15] A. K. Gogoi and R. Raghuram, "Analysis of VLF loop antennas on the Earth surface for underground mine communication," in *Proc. IEEE Antennas Propag. Soc. Int. Symp. Dig.*, Baltimore, MD, USA, May 1996, pp. 962–965.

[16] A. K. Gogoi and R. Raghuram, "Variation of field strength in underground mine area on the size of VLF loop antennas laid on the Earth surface," in *Proc. IEEE Antennas Propag. Soc. Int. Symp.*, Montreal, Quebec, Canada, Dec. 1997, pp. 1792–1795.
[17] K. Li, H.-Q. Zhang, and W.-Y. Pan, "The VLF field on the sea surface generated by the space borne loop antenna," *J. Electromagn. Waves Appl.*, vol. 18, no. 1, pp. 121–135, Apr. 2012, doi: 10.1163/156939304322749715.
[18] L. Kai, "The VLF field on the sea surface generated by the spaceborne loop antenna," in *Proc. Asia–Pacific Microw. Conf.*, Hong Kong, 1997, pp. 1233–1236.
[19] Y.-X. Wang, Z.-W. Zhao, Z.-S. Wu, R.-H. Jin, X.-L. Liang, and J.-P. Geng, "Fast convergence algorithm for earthquake prediction using electromagnetic fields excited by SLF/ELF horizontal magnetic dipole and schumann resonance," *Wireless Pers. Commun.*, vol. 77, no. 2, pp. 1039–1053, Jul. 2014, doi: 10.1007/s11277-013-1553-6.
[20] T. J. Cui, W. C. Chew, X. X. Yin, and W. Hong, "Study of resolution and super resolution in electromagnetic imaging for half-space problems," *IEEE Trans. Antennas Propag.*, vol. 52, no. 6, pp. 1398–1411, Jun. 2004, doi: 10.1109/TAP.2004.829847.
[21] B.-Y. Wu and X.-Q. Sheng, "Acceleration near field interaction in half-space MLFMA by means of genetic algorithm," in *Proc. IEEE Antennas Propag. Soc. Int. Symp. (APSURSI)*, Memphis, TN, USA, Jul. 2014, pp. 753–754.
[22] A. Sommerfeld, "Propagation of waves in wireless telegraphy," *Ann. Phys.*, vol. 28, pp. 665–736, Mar. 1909, doi: 10.1002/andp.19263862516.
[23] A. J. Bańos and J. P. Wesley, "The horizontal electric dipole in a conducting half-space," Marine Phys. Lab., Univ. California, Berkeley, CA, USA, Tech. Rep. 53-33 54-31, 1954, vol. 9.
[24] A. J. Bańos *Dipole Radiation in the Presence of a Conducting Half-Space*. Oxford, U.K.: Pergamon Press, , 1966.
[25] R. W. P. King, M. Owens, and T. T. Wu, *Lateral Electromagnetic Waves: Theory and Applications to Communications* (Geophysical Exploration, and Remote Sensing). New York, NY, USA: Springer-Verlag, 1992.
[26] D. Margetis, "Studies in classical electromagnetic radiation and Bose-Einstein condensation," Ph.D. dissertation, Harvard Univ., Cambridge, MA, USA, 1999.
[27] D. Margetis, "Exactly calculable field components of electric dipoles in planar boundary," *J. Math. Phys.*, vol. 42, no. 2, pp. 713–745, Jan. 2001, doi: 10.1063/1.1330731.
[28] R. E. Collin, "Hertzian dipole radating over a lossy Earth or sea: Some early and late 20th-century controversies," *IEEE Antennas Propag. Mag.*, vol. 46, no. 2, pp. 64–79, Apr. 2004, doi: 10.1109/MAP.2004.1305535.
[29] H. L. Xu, T. T. Gu, Y. Zhu, X. Wei, L. S. Li, and H. C. Yin, "Communication with a magnetic dipole: Near-field propagation from air to undersea," *IEEE Trans. Antennas Propag.*, early access, Aug. 19, 2020, doi: 10.1109/TAP.2020.3016390.
[30] S. Durrani, "Air to undersea communication with magnetic dipoles," *IEEE Trans. Antennas Propag.*, vol. 12, no. 4, pp. 464–470, Jul. 1964, doi: 10.1109/TAP.1964.1138240.
[31] A. C. Fraser-Smith, D. M. Bubenik, and O. G. Villard, "Air/undersea communication at Ultra-Low-Frequencies using airborne loop antennas," Electronics Labs., Stanford Univ., Stanford, CA, USA, Tech. Rep. 6–4207, 1977.
[32] A. C. Fraser-Smith and D. M. Bubenik, "The ULF/ELF/VLF electromagnetic fields generated in a sea of finite depth by elevated dipole sources," Space, Telecommun. Radiosci. Lab., Stanford Univ., Stanford, CA, USA, Tech. Rep. E715-2, 1984.
[33] N. Mohammadi Estakhri, B. Edwards, and N. Engheta, "Inverse-designed metastructures that solve equations," *Science*, vol. 363, no. 6433, pp. 1333–1338, Mar. 2019, doi: 10.1126/science.aaw2498.
[34] N. J. Greybush, V. Pacheco-Peña, N. Engheta, C. B. Murray, and C. R. Kagan, "Plasmonic optical and chiroptical response of self-assembled au nanorod equilateral trimers," *ACS Nano*, vol. 15, pp. 1617–1624, Jan. 2019.
[35] H. L. Xu, T. T. Gu, and K. Li, "Approximated solutions for ELF near-field propagation due to a horizontal electric dipole excitation near the sea-rock boundary," *IEEE Trans. Antennas Propag.*, vol. 66, no. 5, pp. 2471–2481, May 2018, doi: 10.1109/TAP.2018.2810328.
[36] H. L. Xu, T. T. Gu, and H. C. Yin, "ELF wave near-field propagation of a VMD along sea-rock boundary," in *A Closer Look at Magnetic Dipoles*, New York, NY, USA: Nova, 2019, pp. 63–97.

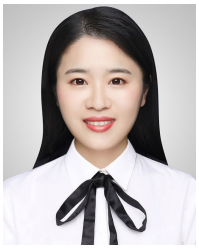

HONGLEI XU (Member, IEEE) was born in Jiangyin, Jiangsu, China, in June 1990. She received the B.S. degree in communication engineering from the Nanjing University of Posts and Telecommunications, Nanjing, China, in 2012, the M.S. degree in communication and information system from Jiangsu University, Zhenjiang, China, in 2015, and the Ph.D. degree in electronic science and technology from Zhejiang University, Hangzhou, China, in 2019.

She is currently working as a Postdoctoral Research Fellow with the Science and Technology on Electromagnetic Scattering Laboratory, Beijing, China. Her current research interests include radio wave propagation theory, radar target characteristics, and electromagnetic scattering modeling.

YONG ZHU was born in Hubei, China. He received the B.S. degree from the Harbin Institute of Technology, Harbin, China, in 1998, and the M.S. degree in electromagnetic field and microwave technique from the Second Academy of the Aerospace Industry Ministry, Beijing, China, in 2001.

He is currently a Senior Researcher with the Science and Technology on Electromagnetic Scattering Laboratory, Beijing Institute of Environmental Features. His current research interests include numerical methods in electromagnetic fields, electromagnetic scattering, and inverse scattering.

XIAO WEI was born in Heilongjiang, China. He received the B.S. degree in electromagnetic field and microwave technique from the Harbin Institute of Technology, Harbin, China, in 2002, the M.S. degree in electromagnetic field and microwave technique from the Second Academy of the Aerospace Industry Ministry, Beijing, China, in 2005, and the Ph.D. degree in electromagnetic field and microwave technique from the Communication University of China, Beijing, in 2013. He is currently a Senior Researcher with the Science and Technology on Electromagnetic Scattering Laboratory, Beijing Institute of Environmental Features. His current research interests include numerical methods in electromagnetic fields and comprehensive application of electromagnetic scattering.

LIANGSHENG LI was born in Nanchang, Jiangxi, China, in 1981. He received the B.S. and M.S. degrees in physics from the Beijing Institute of Technology, in 2003 and 2006, respectively, and the Ph.D. degree in physics from the Institute of Theoretical Physical, Chinese Academy of Sciences, Beijing, China. He is currently a Senior Research Fellow with the Science and Technology on Electromagnetic Scattering Laboratory. His research interests include terahertz wave, metamaterial, quantum radar, and phase transition.

YIN HONG-CHEN was born in Jiangxi, China. He received the B.S. degree in electromagnetic field and microwave technique from the Northwest Telecommunication Engineering Institute, Xi'an, China, in 1986, the M.S. degree in electromagnetic field and microwave technique from the Second Academy of the Aerospace Industry Ministry, Beijing, China, in 1989, and the Ph.D. degree in electromagnetic field and microwave technique from Southeast University, Nanjing, China, in 1993.

He is currently a Senior Researcher with the Science and Technology on Electromagnetic Scattering Laboratory, Beijing Institute of Environmental Features. His current research interests include numerical methods in electromagnetic fields, electromagnetic scattering, inverse scattering, and radar target recognition. He is a Fellow of the Chinese Institute of Electronics.

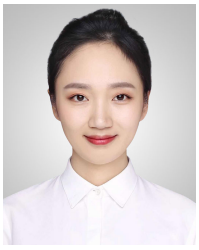

TINGTING GU (Member, IEEE) was born in Leshan, Sichuan, China, in June 1988. She received the B.S. degree in electromagnetic field and microwave technology from the Zhejiang University of Media and Communications, in 2010, the M.S. degree in electromagnetic field and microwave technology from Hangzhou Dianzi University, in 2013, and the Ph.D. degree in electromagnetic field and microwave technology from Zhejiang University, Hangzhou, China, in 2019.

She is currently working as a Postdoctoral Research Fellow in electromagnetic theory and microwave technology with the College of Information Science and Electronic Engineering, Zhejiang University. Her current research interests include radio wave propagation theory and its applications.